VORTEX BREAKDOWN: A TWO-STAGE TRANSITION

M.P. Escudier and J.J. Keller
Brown Boveri Research Centre
CH-5405 Baden, Switzerland

GAMMA/ PI

SUMMARY

It is demonstrated that a large-scale isentropic transition between conjugate swirling flow states can occur with no change in the flow force and that both flow states are supercritical. It is argued that such a transition represents the first stage of vortex breakdown in a tube, the second stage being a non-isentropic transition in the nature of a hydraulic jump to the downstream subcritical state. The intermediate (supercritical) state consists of a zone of stagnant fluid surrounded by a region of potential flow. These two zones are separated by a layer of rotational fluid originating in the upstream vortex core. An outline is given of the analysis for an upstream flow modelled as a Rankine vortex. It is found that for any ratio of core-to-tube radii, breakdown (i.e. the first transition) occurs for a unique value of the swirl number $\Gamma/\pi r U$. In the limiting case of an infitesimally small core, the value is $\sqrt{2}$, compared with the critical value 2·405. It is argued that this limit cannot represent free breakdown, which in consequence must have a different character from the tube-flow breakdowns generally observed.

SQUARE ROOT OF 2

INTRODUCTION

Previous efforts to explain the phenomenon of vortex breakdown have been centred upon the concept of a single transition, either in the sense of Benjamin's [1] conjugate-state analysis or stability theories such as those of Ludwieg [2] and, most recently, Leibovich [3]. For the most part, these efforts have been limited to weak transitions. The experimental evidence reported by Harvey [4], Sarpkaya [5] and others [6,7], in contrast, shows breakdown to be invariably a strong perturbation of the flow, as has been emphasized by, for example, Hall [8] and Leibovich [9]. We present a new and simple approach to the problem of vortex breakdown in tube flow which yields a simple breakdown criterion and is consistent with the observed characteristics of the phenomenon.

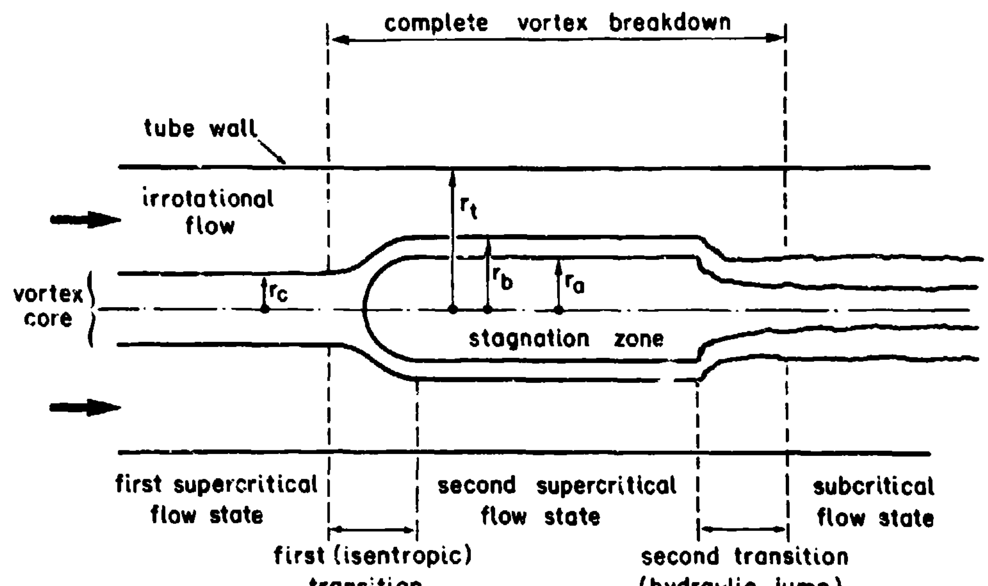

Figure 1. Schematic diagram illustrating the idealized process of vortex breakdown in a cylindrical tube.

The key features of the process of vortex breakdown in a tube are illustrated in figure 1. We propose that the transition may involve two stages, the first isentropic from the initial supercritical state to an intermediate state which is also supercritical. The second stage of the transition, to the downstream subcritical state, is non-isentropic, much like a hydraulic jump or shock wave. The crucial new idea here is that the first transition is both isentropic and also involves no change in the flow force even for a large-scale transition. The latter possibility has been overlooked until recently [10], most significantly by Benjamin [1]. A striking consequence of the analysis is that for a given upstream vortex structure, breakdown occurs only for a unique value of the swirl number $\Gamma/\pi r_c U$ (an inverse Rossby number): e.g. $\sqrt{2}$ for a Rankine vortex with an infinitesimally small core radius r_c. Another prediction is that breakdown is also possible for a purely irrotational swirling flow: the example considered is that of flow in an annulus. Complete details of the analysis are given in two recent papers [10,11] and only the barest essentials are excerpted here to emphasize the principal assumptions and results. We also present the results of a number of experiments in support of the analysis and speculate on the nature of free vortex breakdown and on the real and apparent differences between the axisymmetric and spiral forms of breakdown.

VORTEX BREAKDOWN IN A CYLINDRICAL TUBE - ANALYSIS

A convenient model for the upstream flow state (1) (see figure 1) is the Rankine vortex:

$$v = \begin{cases} \Gamma r/2\pi r_c^2 & \text{if} \quad 0 < r < r_c \\ \Gamma/2\pi r & \text{if} \quad r_c < r < r_t \end{cases} \tag{1}$$

$$w = \text{constant} = U$$

where v and w are the swirl and axial components of velocity, r_c is the core radius, r_t the tube radius and Γ the circulation. The intermediate state (2) is also assumed to be cylindrical with an inner stagnation region of radius r_a separated from the outer potential flow by a layer $r_a < r < r_b$ of rotational fluid originating in the upstream vortex core. The flow between these two states is assumed to be steady, incompressible, axisymmetric and inviscid. The equation governing the intermediate flow state is then [12]

$$\frac{d^2\phi}{dr^2} + \frac{1}{r}\frac{d\phi}{dr} - \frac{\phi}{r^2} = \begin{cases} -k^2\phi & \text{if} \quad r_a < r < r_b \\ 0 & \text{if} \quad r_b < r < r_t \end{cases} \tag{2}$$

where $r\phi$ is the departure of the stream function from its upstream form and

$$k = \Gamma/\pi r_c^2 U . \tag{3}$$

Specification of the intermediate state is completed by introducing appropriate matching conditions at r_a, r_b and r_t, i.e. constancy of the stream function on stream surfaces, continuity of the velocity across the interface $r = r_b$ and zero velocity at $r = r_a$. The solution of equation (2) and calculation of the distributions of v, w and the static pressure p (from $dp/dr = \rho v^2/r$) is then straightforward (see [10] - [12]).

To answer the question which pair of conjugate flow states corresponding to the preceding analysis is physically realistic, we must consider the momentum equation. We define first the flow force S by

$$S = 2\pi\int_0^{r_t}(\rho w^2 + p)r\,dr \tag{4}$$

where ρ is the fluid density. Using the results already obtained, the flow force difference between the first and second flow states may be shown to be

$$\Delta S = \frac{\pi}{4}\rho U^2 k^2 r_c^2[-r_b^2 + \frac{1}{4}(\frac{r_b^4-r_a^4}{r_c^2}) + \frac{3}{4}r_c^2 + \frac{1}{2}r_c^2 \ln(\frac{r_b^2}{r_c^2})]. \tag{5}$$

Since we are considering flow in a cylindrical tube, with no means of applying an external force to the flow, the difference $\Delta S \equiv 0$. The values of kr_c (= $\Gamma/\pi r_c U$) for which this identity is satisfied are plotted in figure 2 as a function of r_c/r_t together with the corresponding critical values of kr_c obtained from [1]

$$\frac{1}{2}\frac{kr_c J_0(kr_c)}{J_1(kr_c)} = \frac{-1}{(r_t/r_c)^2-1} . \tag{6}$$

It is found that the upstream flow (for $\Delta S = 0$) is always supercritical (i.e. kr_c less than the critical value), as is the intermediate flow state which can be demonstrated on the basis of a variational principle [1,10]. As mentioned in the INTRODUCTION, this possibility of a non-trivial supercritical-supercritical transition was only recently recognized [10] and is suggested to be the key to understanding vortex breakdown. For the Rankine vortex, it turns out that for any value of r_c/r_t the first transition occurs for a unique value of kr_c. More generally it may be shown [10] that for given distributions of w(r) and v(r) the speed at which the vortex breakdown structure moves is unique. The subsequent transition to the downstream flow state must be dissipative, and can be treated essentially as a hydraulic jump.

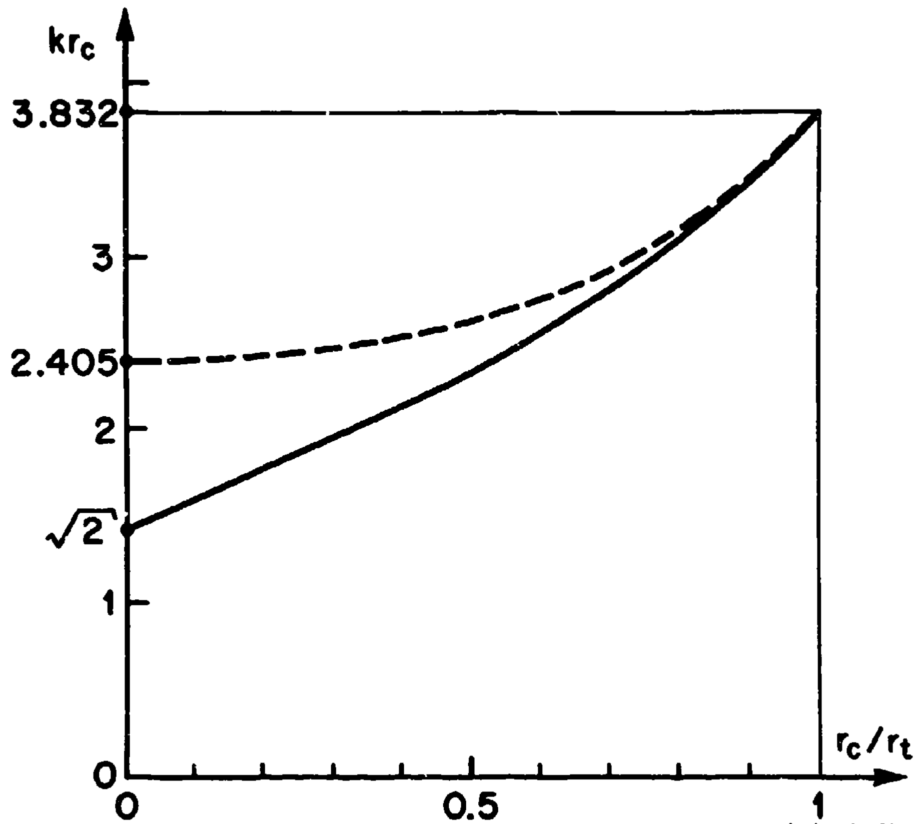

Figure 2. Swirl parameter kr_c for breakdown (solid curve) and critical-flow (broken curve) conditions as a function of normalized core radius.

A remarkable result of the analysis is that a non-trivial transition is predicted even for the asymptotic situation $r_c/r_t \to 0$. In this case

$$\begin{aligned} kr_c &= \sqrt{2} \quad \text{for breakdown} \\ kr_c &= 2{\cdot}405 \quad \text{for the critical state .} \end{aligned} \tag{7}$$

At first sight it might appear that the asymptote $r_c/r_t \to 0$ is relevant to the case of a free vortex ($r_t \to \infty$). However, an asymptotic analysis, which was the subject of [10], shows that this is not the case. In particular, it is found that for $r_c/r_t \to 0$, $r_c/r_b \to 0$ whereas for a free vortex it must be the case that r_c/r_b assumes a value different from zero. It has to be concluded that the free vortex represents a second type of transition compared to that which we have considered, and that this is a direct supercritical - subcritical transition necessarily involving dissipation. A corollary is that investigations of vortex breakdown in tubes are not directly representative of free-vortex breakdown.

Within the small-core approximation, the ideas contained here have been extended to the analysis of general vortex flow in a tube, including the possibility of area changes. In many circumstances it is possible and convenient to relate the actual flow to a fictitious reference Rankine vortex. An interesting result for flows with a strong overshoot in the axial velocity, as is produced by a strong area reduction, is that the critical and breakdown values of kr_c are proportional. This is suggested to be the main reason why Escudier and Zehnder [7] were able to make quite accurate predictions of breakdown on the basis of the criticality condition.

VORTEX BREAKDOWN IN A CYLINDRICAL TUBE - OBSERVATIONS

The two examples of axisymmetric vortex breakdown shown in figure 3 are typical of those reported by Harvey [4], Sarpkaya [5] and others [6,7]. Here advantage has been taken of the laser-induced fluorescence visualisation technique to reveal the inner structure of a breakdown bubble. Fluorescein dye has been injected on the tube axis into the upstream flow. The flow was illuminated by a rapidly oscillating Argon-ion laser beam sweeping through a diametral plane of the tube (further details of the experiment are given in [10] and [13]). Two features may be observed from figure 3 which support the interpretation of vortex breakdown proposed here. First, the fluid entering the bubble in each case clearly emanates from a region much smaller in radius than that of the bubble itself (and also much smaller in radius than the core), and the latter must therefore be a zone of essentially stagnant fluid. Secondly, the smooth appearance of the bubble surface, even when the interior is turbulent, suggests that the first stage of the transition involves little dissipation. It may be remarked that the intermediate state may be masked by spreading of the shear layer at very low Reynolds numbers and by instability and roll up at higher Reynolds numbers.

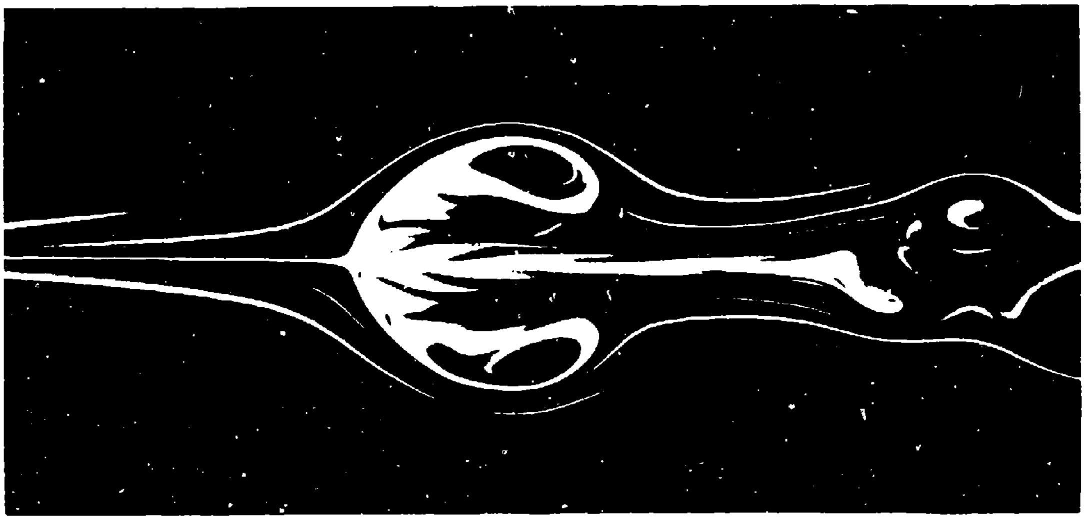

(a) Ur_t/ν = 575

(b) Ur_t/ν = 1650

Figure 3. Examples of vortex breakdown in a cylindrical tube. (Flow from left to right)

The internal structure which may be inferred from flow visualisation is confirmed by laser Doppler anemometry measurements: axial velocity profiles w(r;x) together with the corresponding streamline map for a low Reynolds number breakdown bubble are shown in figure 4. It may be noted that a consequence of the subcritical nature of the flow downstream of such a bubble is that the detailed structure of the bubble itself and the downstream flow are strongly influenced by the downstream geometry and conditions.

The problem of masking of the intermediate flow state, mentioned above, may be overcome by injecting air into the bubble as in the situation shown in figure 5. The smooth character of the first transition is again evident as is the more disturbed nature of the second (the hydraulic jump). The flow conditions are those under which a normal breakdown would occur in the absence of air injection.

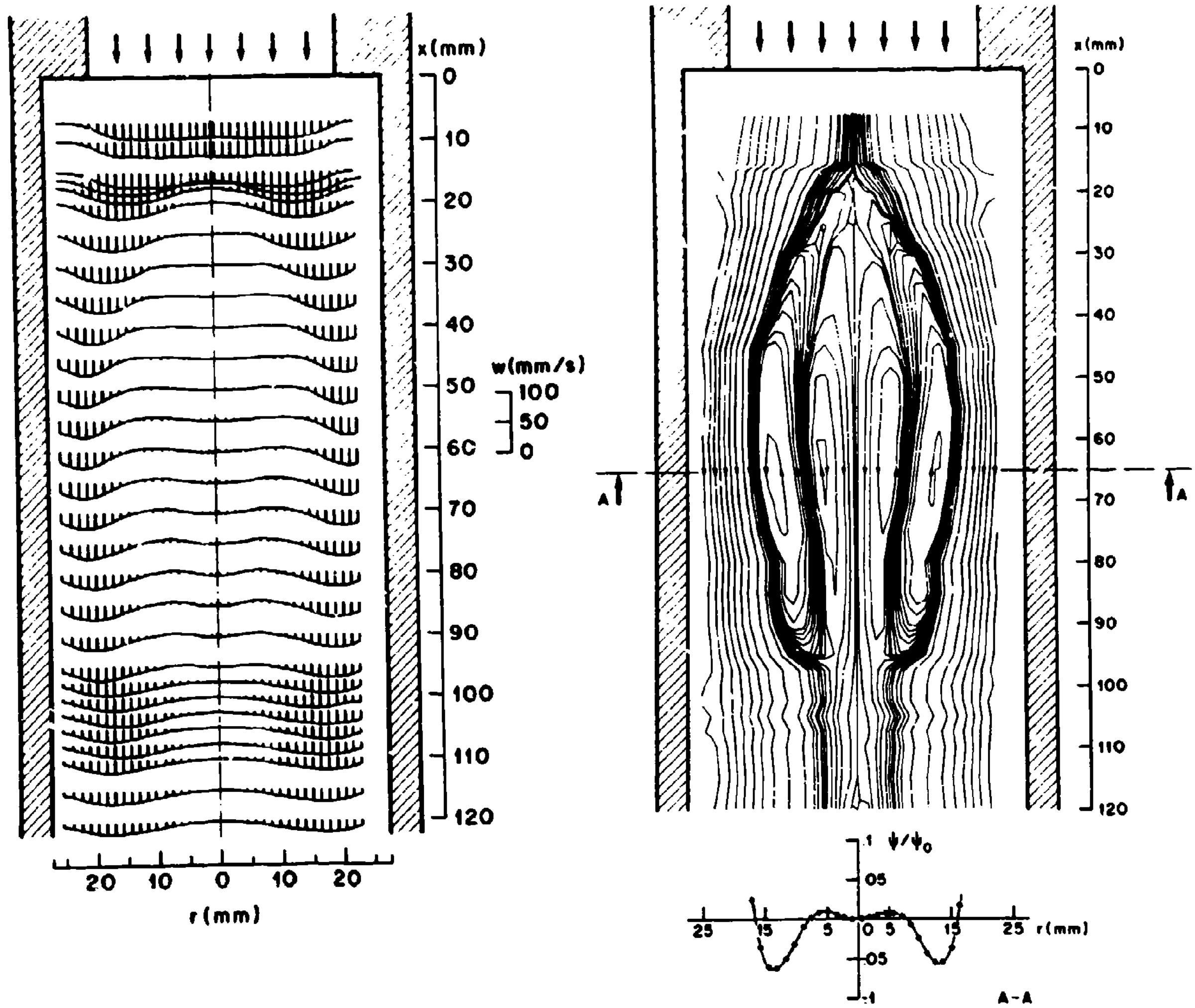

Figure 4. Measured axial velocity profiles $w(r;x)$ and streamline map $\psi(r;x)$ for vortex breakdown in a cylindrical tube with Ur_t/ν = 265.

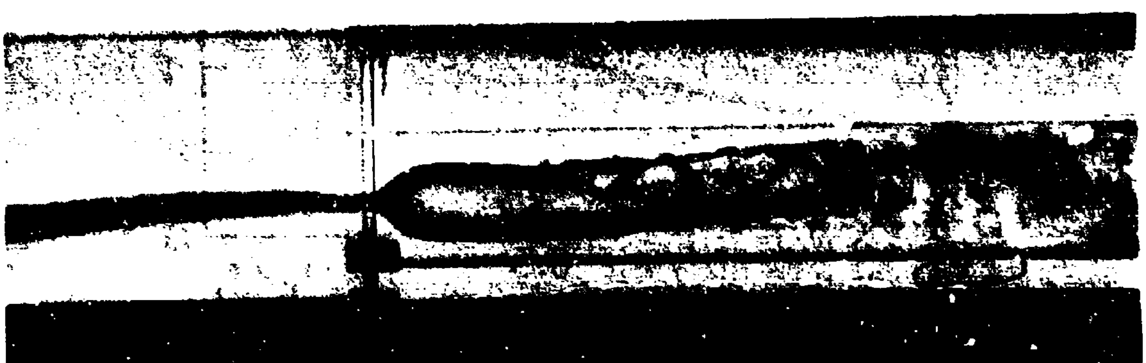

Figure 5. An air-filled vortex-breakdown bubble. (Flow from left to right. Arrows indicate transition locations)

BREAKDOWN OF POTENTIAL FLOW IN AN ANNULUS - ANALYSIS

We consider here a swirling potential flow confined between concentric cylinders. The upstream flow state is defined by

$$v = \Gamma/2\pi r \qquad w = U \qquad r_c < r < r_t \tag{8}$$

i.e. we can imagine the viscous core in figure 1 to be replaced by a solid rod. The second or intermediate flow state is assumed to consist of an annulus of stagnant fluid of outer radius r_b surrounded by a potential vortex

i.e. $v = \Gamma/2\pi r$ and $w = W$ if $r_b < r < r_t$

$v = 0$ and $w = 0$ if $r_c < r < r_b$ (9)

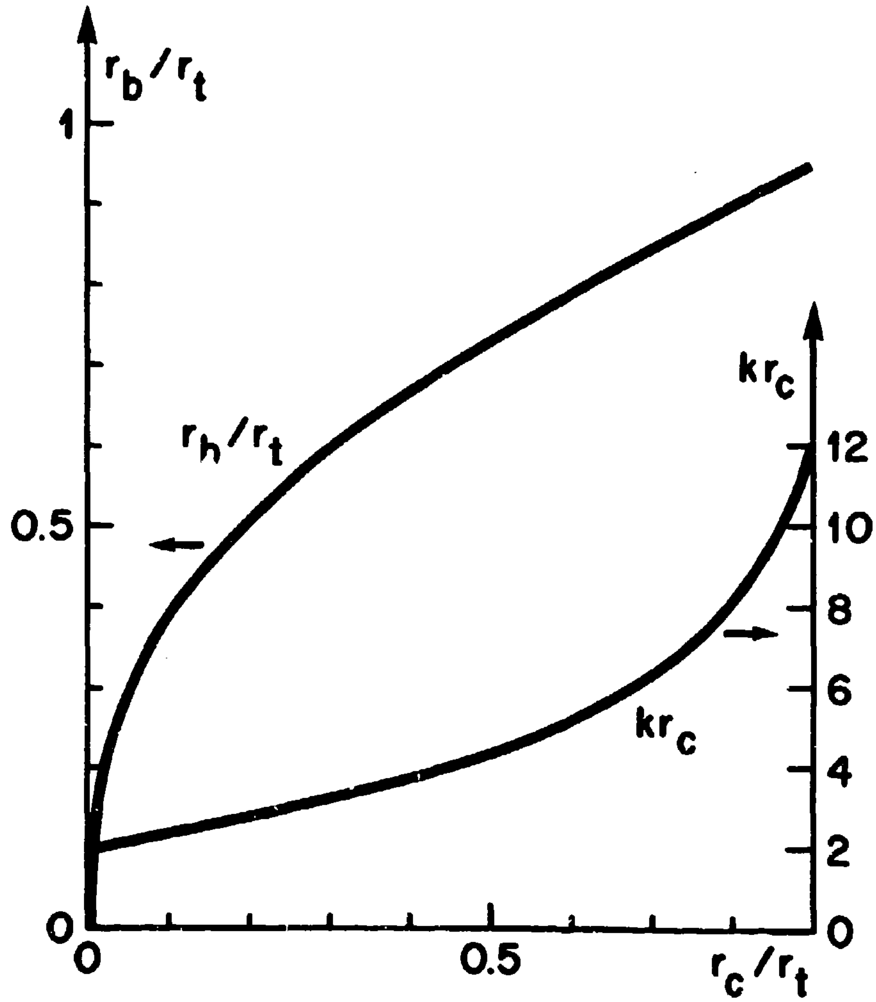

Figure 6. Normalized bubble radius and breakdown swirl parameter kr_c versus normalized inner radius for annular breakdown.

The assumption of an isentropic transition between these two flow states then leads to [10]

$$\left(\frac{r_t^2 - r_c^2}{r_t^2 - r_b^2}\right)^2 = \frac{1}{4}(kr_c)^2\left(1 - \frac{r_c^2}{r_b^2}\right) \tag{10}$$

whilst for the flow-force difference we have

$$\Delta S = \frac{\pi}{2}\rho U^2 r_b^2 \{ [1-(\frac{r_c}{r_b})^2][(\frac{r_t^2-r_c^2}{r_t^2-r_b^2})-\frac{1}{4}(kr_c)^2[1-(\frac{r_c}{r_b})^2+2(\frac{r_c}{r_b})^2 \ell n(\frac{r_c}{r_b})]] \} \tag{11}$$

Setting $\Delta S = 0$ as before leads to kr_c and r_b/r_t as functions of r_c/r_t, as plotted in figure 6. In this case the criticality condition for the downstream flow [14] is

$$(kr_c)^2 = \frac{8r_b^4(r_t^2-r_c^2)^2}{r_c^2(r_t^2-r_b^2)^3} \tag{12}$$

and it is again found that this flow state is always supercritical.

BREAKDOWN OF POTENTIAL FLOW IN AN ANNULUS - OBSERVATIONS

Flow visualisation confirms the occurence of large-scale transitions for swirling flow in an annulus. In the first example (figure 7) multiple breakdowns are evident. Although the viscous core has been "replaced" by a solid rod, viscous influences are undoubtedly responsible for producing the conditions which allow successive breakdowns. The introduction of air into the breakdown region again produces a breakdown bubble similar to that predicted (figure 8). It is found that unless conditions closely match those corresponding to the analysis, air introduced into the flow either penetrates far upstream (kr_c too large) or is swept away (kr_c too small).

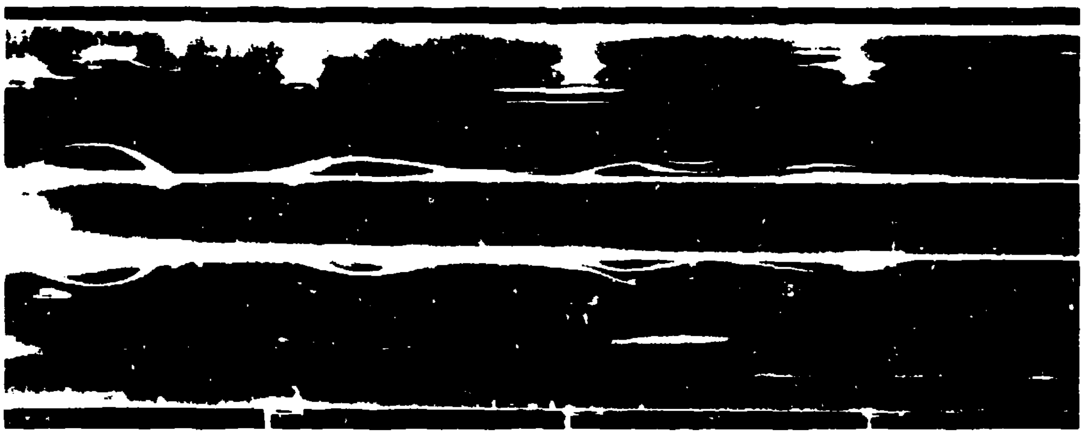

Figure 7. Successive annular breakdowns. (Flow from left to right)

Figure 8. An air-filled annular breakdown. (Flow from left to right)

CONCLUDING REMARKS

The concept proposed here for the explanation of vortex breakdown has been worked out in detail using the Rankine vortex as a model for the upstream flow. The advantage of this formulation is that the equation for the stream function (2) is then linear both within the rotational layer ($r_a < r < r_b$) and also within the surrounding potential flow ($r_b < r < r_t$). As has been indicated, more complex flow situations can be analysed with reference to a fictitious reference Rankine vortex. Such an analysis has been carried out in [10] within the small-core approximation, a restriction which can also be dispensed with as shown in [11]. Any more general analysis would evidently require numerical integration of the equation governing the stream function ψ (the Long [15]-Squire [16] equation) for a cylindrical flow

$$\frac{\partial^2\psi}{\partial r^2} - \frac{1}{r}\frac{\partial\psi}{\partial r} = \frac{r^2}{\rho}\frac{dH}{d\psi} - K\frac{dK}{d\psi} \tag{13}$$

wherein H is the dynamic head and $K = rv$. Such an exercise would undoubtedly provide more accurate results for particular flows, but would be unlikely to contribute significantly to further understanding of the breakdown phenomenon.

We have already speculated that free-vortex breakdown represents a different type of transition to that for tube flow. By way of further speculation we suggest that there is no fundamental difference between the so-called spiral type of breakdown and the axisymmetric bubble type we consider here. The spiral character is suggested to be a consequence of azimuthal instability leading to roll up and detachment of the shear layer surrounding a bubble. This detachment process would then lead to a precessive motion of the near-stagnant interior fluid. Strong evidence in support of this point of view comes from the experiments of Escudier and Zehnder [7] who found the correlation of experimental breakdown data in terms of the simple criterion $\Gamma^2/U\nu L$ = constant to be independent of the breakdown's appearance. It is also well known [8] that the spiral and axisymmetric breakdown forms are found in the same continuous range and are even interchangable under appropriate conditions. A further point is that were the spiral form inherently non-axisymmetric, the spiral would have to remain stationary, as is observed for the non-axisymmetric standing-wave patterns for hollow-core vortices [14].

REFERENCES

1. T.B.Benjamin. Theory of the vortex breakdown phenomenon. J. Fluid Mech. 14, 593-629 (1962).

2. H. Ludwieg. Zur Erklärung der Instabilität der über angestellllten Deltaflügeln auftretenden freien Wirbelkerne. Z. Flugwiss. 10, 242-249 (1962).

3. S. Leibovich. Wave propagation, instability, and breakdown of vortices. In "Vortex Flows", 50-67, Ed. Hornung and Müller, Vieweg (1982).

4. J.K. Harvey. Some observations of the vortex breakdown phenomenon. J. Fluid Mech. 14, 585-592 (1962).

5. T. Sarpkaya. On stationary and travelling vortex breakdowns. J. Fluid Mech. 45, 545-559 (1971).

6. J.H. Faler and S. Leibovich. Disrupted states of vortex flows and vortex breakdown. Phys. Fluids 20, 1385-1400 (1977).

7. M.P. Escudier and N. Zehnder. Vortex flow regimes. J. Fluid Mech. 115, 105-121 (1982).

8. M.G. Hall. Vortex breakdown. Ann. Rev. Fluid Mech. 4, 195-218 (1972).

9. S. Leibovich. The structure of vortex breakdown. Ann. Rev. Fluid Mech. 10, 221-246 (1978).

10. J.J. Keller, M.P. Escudier and J. Bornstein. The physics of vortex breakdown. (1982). Submitted for publication.

11. J.J. Keller. Breakdown of a Rankine vortex. (1983). Submitted for publication.

12. G.K. Batchelor. An introduction to fluid dynamics. Cambridge University Press. (1967).

13. J. Bornstein and M.P. Escudier. LDA measurements within a vortex-breakdown bubble. Proc. Int. Symp. on Applications of Laser Doppler Anemometry. Lisbon, (1982).

14. J.J. Keller and M.P. Escudier. Theory and observations of wave on hollow-core vortices. J. Fluid Mech. 99, 495-511 (1980).

15. R.R. Long. Steady motion around a symmetrical obstacle moving along the axis of a rotating fluid. J. Meteor 10, 197-203 (1953).

16. H.B. Squire. Rotating fluids. In "Surveys in mechanics", 139-161, Ed. Batchelor and Davies, Cambridge University Press (1956).